JACS
JOURNAL OF THE AMERICAN CHEMICAL SOCIETY
Communication
pubs.acs.org/JACS

Modular Artificial Cupredoxins

Samuel I. Mann,[§] Tillmann Heinisch,[‡] Andrew C. Weitz,[†] Michael P. Hendrich,*[,†] Thomas R. Ward,*[,‡] and A. S. Borovik*[,§]

[§]Department of Chemistry, University of California-Irvine, 1102 Natural Sciences II, Irvine, California 92697, United States
[‡]Department of Chemistry, University of Basel, Spitalstrasse 51, CH-4056 Basel, Switzerland
[†]Department of Chemistry, Carnegie Mellon University, Pittsburgh, Pennsylvania 15213, United States

Supporting Information

ABSTRACT: Cupredoxins are electron-transfer proteins that have active sites containing a mononuclear Cu center with an unusual trigonal monopyramidal structure (Type 1 Cu). A single Cu−S_{cys} bond is present within the trigonal plane that is responsible for its unique physical properties. We demonstrate that a cysteine-containing variant of streptavidin (Sav) can serve as a protein host to model the structure and properties of Type 1 Cu sites. A series of artificial Cu proteins are described that rely on Sav and a series of biotinylated synthetic Cu complexes. Optical and EPR measurements highlight the presence of a Cu−S_{cys} bond, and XRD analysis provides structural evidence. We further provide evidence that changes in the linker between the biotin and Cu complex within the synthetic constructs allows for small changes in the placement of Cu centers within Sav that have dramatic effects on the structural and physical properties of the resulting artificial metalloproteins. These findings highlight the utility of the biotin-Sav technology as an approach for simulating active sites of metalloproteins.

Metalloproteins perform a wide range of chemical transformations whose functions have yet to be achieved by artificial systems. The discrepancy in reactivity can be directly linked to the inability of most unnatural systems to duplicate the precise structural control of the primary and secondary coordination spheres that are present within the active sites of proteins. Numerous synthetic systems and artificial metalloproteins (ArMs) have been developed to regulate both coordination spheres, and notable successes have been achieved.[1−9] Biotin-streptavidin (Sav) technology has been found to be an effective method for placing metal complexes in specific locations within a protein thanks to Sav's unusually high affinity for biotin (K_b > 10^{14} M^{-1}).[10] For instance, ArMs comprised of biotinylated organometallic complexes and Sav catalyze a variety of organic transformations, many of which having impressive selectivities.[11,12] We have extended this approach toward developing artificial Cu-proteins whose primary and secondary coordination sphere can be systematically modulated. We show herein that biotinylated Cu complexes can be confined within Sav to prepare ArMs that have properties similar to those of cupredoxins.

Cupredoxins have a central role in biological electron-transfer processes and contain active sites with a single copper center (referred to as Type I Cu centers, Figure 1A) with unusual structural and spectroscopic properties and relatively high redox potentials (180−800 mV vs NHE).[3,13] Detailed structure−function studies have found that "classic" Type 1 centers, such as that in *Alcaligenes denitrificans* azurin, have Cu sites with unique coordination geometries that are best characterized as distorted trigonal monopyramidal. The trigonal plane contains two N atom donors from histidine residues and one S atom donor from a cysteine thiolate; the axial ligand can vary but is often an S atom from a methionine thioether that only weakly interacts with the Cu center (Cu−S_{met} > 2.8 Å). The highly covalent Cu^{II}−S(thiolate) bond is responsible for the distinct color that arises from an intense S_π−Cu ligand-to-metal charge transfer band at λ_{max} ∼ 600 nm (ε_M = 3000−6000) as well as the small Cu hyperfine coupling of A_z ∼ 180 MHz. Variations within cupredoxins exist that are manifested in different structural and spectroscopic properties. These "perturbed" sites (e.g., *Rhus vernicifera* stellacyanin) have an absorbance band at λ_{max} ∼ 600 nm but exhibit an additional feature at λ_{max} ∼ 450 nm.[14,15] Solomon has defined the parameter $R\varepsilon = \varepsilon_{450}/\varepsilon_{600}$ to distinguish between the various Type 1 Cu sites: an $R\varepsilon$ of <0.15 is considered a classical site, whereas those with larger values are perturbed sites.[13] In addition to their unique primary coordination spheres, the secondary coordination spheres about the Cu centers in cupredoxins impact function. These effects are elegantly illustrated in the work of Lu who used mutagenesis methods to re-engineer the active site in azurin to vary the reduction potential by nearly 2 V.[9]

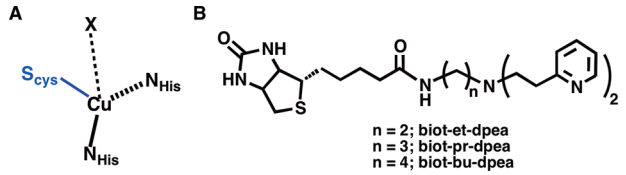

Figure 1. Primary coordination sphere of Type 1 Cu center (A) and biotinylated ligands used in this study (B).

It has been a challenge to reproduce the structural, spectroscopic, and redox properties of Type 1 Cu sites within artificial systems. Attempts to model these active sites include metallopeptides with sequences that contain the loop of

Received: May 26, 2016
Published: July 6, 2016

DOI: 10.1021/jacs.6b05428
J. Am. Chem. Soc. 2016, 138, 9073−9076

cupredoxins[16] and three-helix bundles[17] that assemble to form a Type 1 Cu binding site. In addition, synthetic Cu complexes have been prepared with sterically constrained ligands that have been useful in investigating the details of the Cu^{II}–S(thiolate) interaction.[18−20] However, there are few synthetic examples that can simulate the properties of Type 1 Cu sites, and none that incorporate a biologically relevant S-donor from cysteine.

We selected the biotinylated di[2-(2-pyridyl)ethyl]amine (dpea), which is a tridentate ligand that Karlin has shown to tightly bind to Cu^{II} ions.[21] Three constructs were prepared that differed by the linker group between the biotin and dpea (biot-R-dpea, where R = et, pr, bu) via a 3-step route from dpea (Scheme S1). Formation of the Cu^{II} complexes was achieved by treating biot-R-dpea with $CuCl_2$ in CH_3CN to afford $[Cu^{II}$(biot-R-dpea)$(Cl)(H_2O)]Cl$. The ArMs $[Cu^{II}$(biot-R-dpea)$(H_2O)_2]^{2+}$⊂Sav WT (R = et (**1a**); pr (**1b**); bu (**1c**)) were prepared by incubating Sav WT at pH 6 in MES buffer (50 mM) with a DMF solution of $[Cu^{II}$(biot-R-dpea)$(Cl)(H_2O)]Cl$ for 5 min. A 4:1 ratio of each $[Cu^{II}$(biot-R-dpea)$(Cl)(H_2O)]Cl$ complex to Sav WT was determined using the (2-(4′-hydroxyazo-benzene)benzoic acid assay[22] (Figure S1), indicating that each subunit contains one Cu complex. The spectroscopic properties support the formation of the artificial Cu proteins; protein solutions have weak bands at $\lambda_{max} \sim 650$ ($\varepsilon_M \sim 50$) that are assigned to d–d transitions for the immobilized Cu(II) centers (Figures 2 and S2A, Table S1). The EPR spectra

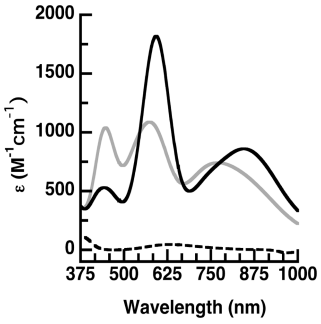

Figure 2. Absorbance spectra for **1a** (---), **2a** (gray), and **2b** (black).

for **1a–c** are nearly identical and were simulated for species with $S = 1/2$ spin ground states. In addition, each spectrum contained two sets of signals of equal intensity (Figure S3) that we suggest are caused by the immobilized Cu(II) complex adopting two orientations (Table S1).

Single crystals of **1a** were prepared by soaking crystals of apo-Sav WT with $[Cu^{II}$(biot-et-dpea)$(H_2O)_2]^{2+}$. Its structure was solved to 1.72 Å resolution[23] to reveal a single Cu(II) complex housed within each subunit of Sav WT arranged in a trigonal bipyramidal geometry, in which the primary coordination sphere is composed of 3 nitrogen atoms from the dpea ligand and 2 oxygen donors from aquo ligands (Figure S4A, Table S2). The dpea ligand binds in a meridional fashion to the copper center with an average Cu–N bond length of 1.98(1) Å.[24] Note that O1 is also part of an H-bonding network that includes S112, the carbonyl of A86, and a structural water molecule.

The structural results for **1a** indicate that targeting position 112 may offer a suitable site to install an endogenous donor that could bind to the immobilized Cu complex. Previous work has shown that the imidazole residue in the $S_{112}H$ variant can coordinate to and immobilize a biotinylated Rh complex.[25] Rather than using $S_{112}H$ as the host, we prepared new artificial Cu proteins using the $S_{112}C$ variant with the goal to design ArMs with Cu sites that are similar to those found in cupredoxins. The confinement of complexes within a subunit should prevent intermolecular interactions that often hinder the formation of discrete Cu–S_{cys} complexes in synthetic systems. For instance, reactions with free $[Cu^{II}$(biot-pr-dpea)$(H_2O)Cl]Cl$ complex and various thiols, including the cysteine derivative *N*-(*tert*-butoxycarbonyl)-L-cysteine methyl ester in DMF, led to a loss of the Cu^{II} complex presumably through reduction and formation of disulfide species (Figure S5). To form discrete and stable complexes with Cu–S_{cys} bonds, the $S_{112}C$ variant was incubated with $[Cu^{II}$(biot-R-dpea)$(Cl)(H_2O)]Cl$ using the conditions described above for Sav WT to produce $[Cu^{II}$(biot-R-dpea)$S_{cys112}]^+$⊂Sav $S_{112}C$ (R = et, (**2a**), pr, (**2b**), bu, (**2c**)).

ArM **2a** exhibited optical features that were significantly different from those of **1** with an electronic absorption spectrum containing intense bands at λ_{max} (ε_M) = 445 (1020), 570 (1010), and 770 (700) (Figure 2, Table 1). These data produced an $R\varepsilon$ =

Table 1. Properties for 2a–c and Selected Cupredoxins

	S112C				
host n	et (**2a**)	pr (**2b**)	bu (**2c**)	stellacyanin[a]	azurin $M_{121}H$[b,c]
λ_{max}, nm (ε_M)	448 (1040)	443 (530)	437 (780)	440 (1090)	439 (NR)
	574 (1090)	593 (1820)	611 (1790)	595 (4970)	593 (NR)
	771 (740)	846 (860)	891 (840)	781(690) 893(580)	
$R\varepsilon$	0.95	0.29	0.44	0.22	1.8
g	2.02	2.05	2.06	2.02	2.05
	2.07	2.06	2.08	2.08	2.05
	2.19	2.18	2.19	2.29	2.25
A, MHz	nd, nd	17	4	171	27, 27
	353	264	225	87	305
		71	79	105	
$E_{1/2}$ mV[d]	140	110	95	184	<200

[a]Refs 14, 26, and 27. [b]Ref 28. [c]pH = 6. [d]NHE, rt, 50 mM MES pH 6.

0.95, which is similar to the value of 0.82 reported for the purple cupredoxin Nmar1307.[29] Structural information obtained from XRD studies on **2a** supports thiolate coordination. Analysis of single crystals that diffracted to 1.70 Å resolution revealed formation of a mononuclear Cu complex within each subunit in which the Cu center has an N_3S primary coordination sphere (Figure S4B). The dpea ligand adopts a facial orientation around the immobilized Cu center in **2a** producing an average Cu–N bond distance of 2.10(2) Å and a Cu–S1 bond length of 2.18(2) Å (Table 2). The Cu^{II} complex has N1–Cu–N2, S1–Cu–N1, and S1–Cu–N2 bond angles of 92(3)°, 129(2)°, and 113(2)° that form a distorted trigonal plane with the Cu positioned 0.62 Å from the plane. In addition, a relatively long N2–Cu–N3 bond angle of 127(2)° was observed.

More intense bands at $\lambda_{max} \sim 600$ nm were obtained for **2b** and **2c**, and the higher energy bands at $\lambda_{max} \sim 445$ nm were weaker in intensity compared to **2a** (Figure 2, Table 1).

These new optical data produce $R\varepsilon$ values of 0.29 for **2b** and 0.44 for **2c**, both of which are significantly lower than that in **2a** and are approaching values that normally are associated with classical blue copper sites. Structural studies on **2b** support that the Cu centers in these ArMs are distinct from that in **2a** and more comparable to classical Type I Cu sites. The molecular

DOI: 10.1021/jacs.6b05428
J. Am. Chem. Soc. 2016, 138, 9073−9076

Table 2. Selected Bond Lengths (Å) and Angles (deg) for 2a−c, Stellacyanin, and $M_{121}H$ Azurin

	$S_{112}C$				
host n	et (**2a**)	pr (**2b**)	bu (**2c**)	stellacyanin[b]	azurin, $M_{121}H$[c,d]
Cu−N1	2.19(2)	2.24(2)	2.28(2)	2.04(2)	2.02(1)
Cu−N2	2.03(2)	2.05(2)	2.10(2)	1.96(2)	2.06(1)
Cu−N3	2.09(2)	2.20(2)	2.12(2)	–	2.24(1)
Cu−S1	2.18(2)	2.11(2)	2.09(2)	2.18(2)	2.25(1)
d[Cu−$(N/S)_t$][a]	0.62	0.41	0.66	0.32	0.58
N1−Cu−N2	92(3)	92(3)	89(3)	101(3)	98(3)
N1−Cu−S1	129(3)	124(3)	124(3)	118(3)	109(3)
N2−Cu−S1	113(3)	132(3)	118(3)	134(3)	130(3)
N1−Cu−N3	97(3)	94(3)	87(3)	–	126(3)
N2−Cu−N3	127(3)	96(3)	105(3)	–	89(3)
N3−Cu−S1	100(3)	110(3)	124(3)	–	106(3)

[a]Distance of Cu from trigonal plane. [b]Ref 30. [c]Ref 31. [d]pH 6.

structure of **2b** from XRD data collected to 1.70 Å resolution, again, revealed a mononuclear, 4-coordinate Cu complex with an N_3S primary coordination sphere (Figure 3A). However,

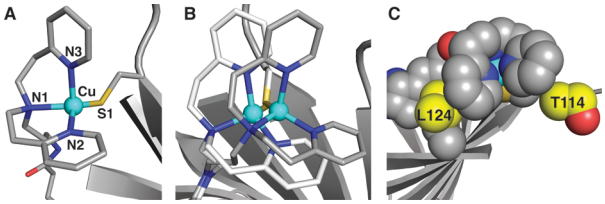

Figure 3. Structure of **2b** (A), structural overlay of **2a** (white) and **2b** (gray) (B), and space-filling representation of **2b** highlighting interactions with residues (yellow) of the protein host (C).

noticeable differences were observed in the structure of the Cu complex in **2b** compared to those in **2a**. The Cu center in **2b** is positioned 1.3 Å further from the biotin binding site, an adjustment that places the pyridine ring containing N2 nearer to residue L124 and that places N3 nearer to residue T114 (Figure 3C). To avoid steric clashing, a significant contraction of the N2−Cu−N3 angle results from 127° in **2a** to 96° in **2b** (Table 2). These changes in structure for **2b** result in an immobilized trigonal monopyramidal Cu complex that has similar properties to Type I Cu centers. For instance, the N1−Cu−N2, S1−Cu−N1, and S1−Cu−N2 bond angles of 92(3)°, 124(2)°, and 132(2)° are nearly equivalent to the related angles found in azurin $M_{121}H$[31] and stellacyanin (Table 2).[30] In addition, the Cu−S1 bond length in **2b** has contracted to 2.11(2) Å, and the Cu center is displaced only 0.41 Å from the trigonal plane, which is closer to those found in Type 1 Cu sites (Table 2). We have also solved the molecular structure of **2c** to 1.40 Å resolution, and the structure of the Cu complex is similar, but not identical to **2b,** (Table 2, Figure S4D) with the Cu center moving 0.82 Å further from the biotin binding site.

The properties of **2a−c** determined from S- and X-band EPR spectroscopy exhibited considerable differences in comparison to ArMs with Sav WT as the host (**1a−c**) (Figure 4).[32,33] New methods we introduce here use the spectra from two microwave frequencies, paired with simulation, to determine the A-tensors in the absence of resolved hyperfine splittings. The EPR spectra for **2a** showed a 4-line hyperfine pattern at g_z = 2.19 with a reduced A_z value of 353 MHz compared to the average A_z value of 523 MHz obtained for **1a**. The lowering of the A_z-value in **2a** is consistent with Cu−S_{cys} interaction in the ArM. The EPR spectra

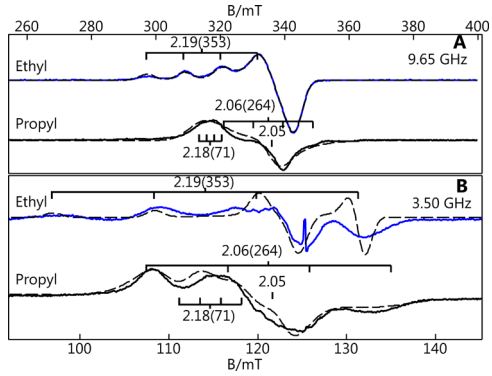

Figure 4. X- (A) and S-band (B) difference EPR spectra for **2a** (blue) and **2b** (black). Simulations are dashed lined. Minor amounts of WT ArMs were subtracted from each spectrum.[33] The g-values and (A-values in MHz) as indicated.

for **2b** and **2c** are dramatically different from that of **2a**. Normally for Cu(II) complexes, the large hyperfine splitting for $A_z = A_\parallel$ is associated with $g_z = g_\parallel$. This is not the case for **2b** and **2c**, in which the g_z-values of 2.18 and 2.19 have associated A_z-values that are low (71 or 79 MHz, respectively). The largest hyperfine splitting values were found in the perpendicular direction: A_y-values of 264 (**2b**) and 225 MHz (**2c**) were determined from our simulations with A_x-values closer to zero (Table 1). These values indicate a rhombic A-tensor that deviates significantly from axial symmetry, in contrast to the g-tensor that is nearly axial. The combination of low A_z-values and rhombic A-tensors for **2b** and **2c** is rare and is directly linked to their protein-induced coordination spheres. The small A_z-value for **2b** and **2c** is indicative of relatively large covalency that is consistent with the short Cu−S_{cys} bond lengths observed in the XRD studies.[20] The rhombic A-tensor indicates a significant admixture of the d_{z^2} orbital into the singly occupied $d_{x^2-y^2}$. Our findings for **2b** and **2c** are similar to those reported for stellacyanin and the $M_{121}H$ variant of azurin (Table 1).[28]

The redox properties of the Cu ArMs were measured using cyclic voltammetry (Figure S6): **1a** contains a reversible one-electron process for the Cu(II)/(I) couple at $E_{1/2}$ = 70 mV versus NHE that shifts to 140 mV in **2a**. This positive shift for the $S_{112}C$ variant is expected for a thiolate-ligated Cu center, and the potential of 140 mV approaches those reported for Type I proteins. The CVs of **1b−c** and **2b−c** are less reversible than **1a** and **2a** but exhibit a similar trend with an increase in E_a of ∼70 mV for **2b** versus **1b** and ∼35 mV for **2c** versus **1c** (Figure S7).

DOI: 10.1021/jacs.6b05428
J. Am. Chem. Soc. 2016, 138, 9073−9076

This shift to positive potentials most likely reflects a more covalent Cu−S_{cys} bond in **2b** and **2c**.

The results for our artificial Cu proteins revealed important design features for using Sav to confine coordination complexes. ArMs with Sav WT produced Cu complexes having nearly identical properties that are similar to those found in synthetic Cu species. However, the $S_{112}C$ variant of Sav produced artificial Cu proteins **2a−c** that have markedly different properties caused by the presence of an endogenous thiolate ligand. Moreover, we were able to tune the position of the Cu centers within Sav $S_{112}C$ by varying the linker between the biotin and the metal complex that produced commensurate changes in the properties of the Cu complexes. This method was ineffective with Sav WT in which the linker length had little effect on the confined species, suggesting that one-point binding through the biotin-Sav interaction may not be enough to regulate the placement of a metal complex within Sav. Coupling the ability to vary the linker with additional anchoring via endogenous ligand coordination offers a versatile means to fine-tune the properties of the metal cofactors.

The properties of **2b** and **2c** also illustrate the potential of this approach to model active sites of metalloproteins. The ability to modify the Sav host to engineer endogenous ligands, combined with synthetic ligands, produces new types of coordination spheres around the immobilized Cu centers that cannot be readily accessed in a pure synthetic construct. The formation of stable complexes with discrete Cu−S_{cys} bonds in **2a−c** was achieved by taking advantage of a Sav variant as the protein host. These results further highlight the benefits of this approach in modulating the structure and properties of an immobilized metal complex to obtain new structures.

■ ASSOCIATED CONTENT

Supporting Information

The Supporting Information is available free of charge on the ACS Publications website at DOI: 10.1021/jacs.6b05428.

Experimental details for all reactions, physical and XRD measurements, Figures S1−S8, and electron density overlays for all protein structures (PDF)

■ AUTHOR INFORMATION

Corresponding Authors

*aborovik@uci.edu
*thomas.ward@unibas.ch
*hendrich@andrew.cmu.edu

Notes

The authors declare no competing financial interest.

■ ACKNOWLEDGMENTS

The authors thank the NIH (GM50781-21S1 to A.S.B. and T.R.W. and GM77387 to M.P.H.) for financial support. We thank T. Poulos, H. Li, and J. Klehr for assistance.

■ REFERENCES

(1) Cook, S. A.; Borovik, A. S. *Acc. Chem. Res.* **2015**, *48*, 2407.
(2) Shook, R. L.; Borovik, A. S. *Inorg. Chem.* **2010**, *49*, 3646.
(3) Liu, J.; Chakraborty, S.; Hosseinzadeh, P.; Yu, Y.; Tian, S.; Petrik, I.; Bhagi, A.; Lu, Y. *Chem. Rev.* **2014**, *114*, 4366.
(4) DeGrado, W. F.; Summa, C. M.; Pavone, V.; Nastri, F.; Lombardi, A. *Annu. Rev. Biochem.* **1999**, *68*, 779.
(5) Bos, J.; Browne, W. R.; Driessen, A.; Roelfes, G. *J. Am. Chem. Soc.* **2015**, *137*, 9796.
(6) Marchi-Delapierre, C. M.; Rondot, L.; Cavazza, C.; Ménage, S. *Isr. J. Chem.* **2015**, *55*, 61.
(7) Song, W. J.; Tezcan, F. A. *Science* **2014**, *346*, 1525.
(8) Berggren, G.; Adamska, A.; Lambertz, C.; Simmons, T. R.; Esselborn, J.; Atta, M.; Gambarelli, S.; Mouesca, J. M.; Reijerse, E.; Lubitz, W.; Happe, T.; Artero, V.; Fontecave, M. *Nature* **2013**, *499*, 66.
(9) Hosseinzadeh, P.; Marshall, N. M.; Chacón, K. N.; Yu, Y.; Nilges, M. J.; New, S. Y.; Tashkov, S. A.; Blackburn, N. J.; Lu, Y. *Proc. Natl. Acad. Sci. U. S. A.* **2016**, *113*, 262.
(10) Weber, P. C.; Ohlendorf, D. H.; Wendoloski, J. J.; Salemme, F. R. *Science* **1989**, *243*, 85.
(11) Wilson, M. E.; Whitesides, G. M. *J. Am. Chem. Soc.* **1978**, *100*, 306.
(12) Dürrenberger, M.; Ward, T. R. *Curr. Opin. Chem. Biol.* **2014**, *19*, 99.
(13) Solomon, E. I.; Hadt, R. G. *Coord. Chem. Rev.* **2011**, *255*, 774.
(14) LaCroix, L. B.; Randall, D. W.; Nersissian, A. M.; Hoitink, C. W. G.; Canters, G. W.; Valentine, J. S.; Solomon, E. I. *J. Am. Chem. Soc.* **1998**, *120*, 9621.
(15) Olesen, K.; Veselov, A.; Zhao, Y.; Wang, Y.; Danner, B.; Scholes, C. P.; Shapleigh, J. P. *Biochemistry* **1998**, *37*, 6086.
(16) Daugherty, R. G.; Wasowicz, T.; Gibney, B. R.; DeRose, V. J. *Inorg. Chem.* **2002**, *41*, 2623.
(17) Plegaria, J. S.; Duca, M.; Tard, C.; Friedlander, T. J.; Deb, A.; Penner-Hahn, J. E.; Pecoraro, V. L. *Inorg. Chem.* **2015**, *54*, 9470.
(18) Kitajima, N.; Fujisawa, K.; Tanaka, M.; Moro-oka, Y. *J. Am. Chem. Soc.* **1992**, *114*, 9232.
(19) Holland, P. L.; Tolman, W. B. *J. Am. Chem. Soc.* **1999**, *121*, 7270.
(20) Randall, D. W.; George, S.; Hedman, B.; Hodgson, K. O.; Fujisawa, K.; Solomon, E. I. *J. Am. Chem. Soc.* **2000**, *122*, 11620.
(21) Karlin, K. D.; Kaderli, S.; Zuberbühler, A. D. *Acc. Chem. Res.* **1997**, *30*, 139−147.
(22) Skander, M.; Humbert, N.; Collot, J.; Gradinaru, J.; Klein, G.; Loosli, A.; Sauser, J.; Zocchi, A.; Gilardoni, F.; Ward, T. R. *J. Am. Chem. Soc.* **2004**, *126*, 14411.
(23) Crystals of **1b** and **1c** did not provide suitable data.
(24) Thyagarajan, S.; Murthy, N. N.; Sarjeant, A. A. N.; Karlin, K. D.; Rokita, S. E. *J. Am. Chem. Soc.* **2006**, *128*, 7003.
(25) Zimbron, J. M.; Heinisch, T.; Schmid, M.; Hamels, D.; Nogueira, E. S.; Schirmer, T.; Ward, T. R. *J. Am. Chem. Soc.* **2013**, *135*, 5384.
(26) Malmström, B. G.; Reinhammar, B.; Vänngård, T. *Biochim. Biophys. Acta, Bioenerg.* **1970**, *205*, 48.
(27) Reinhammar, B. R. *Biochim. Biophys. Acta, Bioenerg.* **1972**, *275*, 245.
(28) Kroes, S. J.; Hoitink, C. W.; Andrew, C. R.; Ai, J.; Sanders-Loehr, J.; Messerschmidt, A.; Hagen, W. R.; Canters, G. W. *Eur. J. Biochem.* **1996**, *240*, 342.
(29) Hosseinzadeh, P.; Tian, S.; Marshall, N. M.; Hemp, J.; Mullen, T.; Nilges, M. J.; Gao, Y.-G.; Robinson, H.; Stahl, D. A.; Gennis, R. B.; Lu, Y. *J. Am. Chem. Soc.* **2016**, *138*, 6324.
(30) Hart, P. J.; Nersissian, A. M.; Herrmann, R. G.; Nalbandyan, R. M.; Valentine, J. S.; Eisenberg, D. *Protein Sci.* **1996**, *5*, 2175.
(31) Messerschmidt, A.; Prade, L.; Kroes, S. J.; Sanders-Loehr, J.; Huber, R.; Canters, G. W. *Proc. Natl. Acad. Sci. U. S. A.* **1998**, *95*, 3443.
(32) Lancaster, K. M.; Zaballa, M.-E.; Sproules, S.; Sundararajan, M.; DeBeer, S.; Richards, J. H.; Vila, A. J.; Neese, F.; Gray, H. B. *J. Am. Chem. Soc.* **2012**, *134*, 8241.
(33) All EPR spectra of the Cu ArMs with $S_{112}C$ contained varying amounts (20−50%) species with features the same as those found in **1a−c** that were subtracted from the spectra in Figure 4. Complete details are found in the SI.

DOI: 10.1021/jacs.6b05428
J. Am. Chem. Soc. 2016, 138, 9073−9076